

The influence of elastic mismatch on the size of the plastic zone of a crack terminating at a brittle-ductile interface

ALBERTO ROMEO and ROBERTO BALLARINI

Department of Civil Engineering, Case Western Reserve University, Cleveland, Ohio 44106-7201, USA

Received 20 June 1993; accepted in final form 27 October 1993

Abstract. This paper presents the results of an investigation of the effects of elastic mismatch on the size of the plastic zone at the tip of cracks terminating at a bimaterial interface. Using the Williams technique, an asymptotic solution is obtained for the magnitude of the crack tip stress singularity λ and for the stress field associated with a semi-infinite crack impinging on an interface. This solution, together with the Von Mises yield criterion, is used to estimate the location of the plastic zone boundary r_0 for various levels of the elastic mismatch, which are expressed in terms of the Dundurs constants. Results are expressed in terms of the non-dimensional quantity

$$r_0 \left[\frac{1}{\sqrt{2\pi}} \frac{k_I}{\sigma_0} \right]^{-1/\lambda},$$

where k_I is the stress intensity factor and σ_0 is the yield stress. These results, together with an integral equation solution for k_I , are used to calculate the size of the plastic zone of a crack of length $2a$ loaded by uniform pressure. It is shown that the location of the boundary of the plastic zone depends strongly on the elastic mismatch.

1. Introduction

Metal-matrix composites reinforced with ceramic particles or fibers and laminated composites comprised of alternate layers of ceramics and metals are examples of systems that rely on the advantages obtained by combining brittle and ductile constituents. The mechanisms that contribute to toughening in such systems include crack trapping, crack bridging, crack shielding, and crack tip plasticity. In most cases toughening results in resistance-curve (*R*-curve) characteristics, wherein the fracture resistance increases with increasing crack length. The resistance to crack growth can be strongly influenced by the microstructure and by the properties of the constituents. In this paper an approximate model is developed that provides qualitative information about the effects of *elastic* mismatch on the size of the plastic zone at the tip of a *finite length* crack that meets an interface between two dissimilar materials. Under the assumption of small scale yielding conditions, an asymptotic elastic analysis is used to calculate the dominant elastic stress field in the vicinity of the crack tip. These stresses are used in conjunction with the Von Mises yield criterion to estimate the location of the elastic-plastic boundary in the ductile material. It is shown that the results for a generic crack can be presented in terms of the parameter

$$r_0 \left[\frac{1}{\sqrt{2\pi}} \frac{k_I}{\sigma_0} \right]^{-1/\lambda} = R_0(\theta; \alpha, \beta),$$

where α and β are the Dundurs parameters, θ is the polar angle measured with respect to the crack plane, k_I is the stress intensity factor, λ is the strength of the stress singularity and σ_0 is the yield stress. The calculated results indicate that R_0 is a strong function of the Dundurs parameters, as it has also been shown by He et al. [1] using the finite element method. However, to evaluate the size of the plastic zone in the yielding material, the stress intensity factor at the interface must be determined for each level of elastic mismatch; in fact, for a bimaterial system k_I not only depends on geometry and loading (as in the case of homogeneous systems) but it is strongly influenced by the Dundurs parameters. As an application, the size of the plastic region induced at the interface by a Griffith crack loaded by uniform pressure is evaluated.

In the next section Zak and Williams' [2] asymptotic analysis of a semi-infinite crack that touches a bimaterial interface is rederived, and the results are used to calculate R_0 . The third section presents a singular integral equation solution for the stress intensity factors of a Griffith crack terminating at a bimaterial interface. These are used to study the effects of elastic mismatch on the location of the elastic-plastic boundary.

2. Asymptotic analysis

The asymptotic problem analyzed is shown in Fig. 1. A mode I semi-infinite crack terminates at the interface between two elastic isotropic half-planes with shear moduli μ_i and Poisson's ratios ν_i ($i = 1, 2$). Following Zak and Williams [2] the stress state associated with this problem is derived from a pair of Airy stress functions $\chi^{(i)}(r, \theta)$ whose general form in polar coordinates can be written as

$$\chi^{(i)}(r, \theta) = \{A_1^{(i)} \cos(\lambda - 2)\theta + A_2^{(i)} \sin(\lambda - 2)\theta + A_3^{(i)} \cos \lambda\theta + A_4^{(i)} \sin \lambda\theta\} r^{2-\lambda}; \quad i = 1, 2, \quad (1)$$

where superscript (i) denotes 'in material i '.

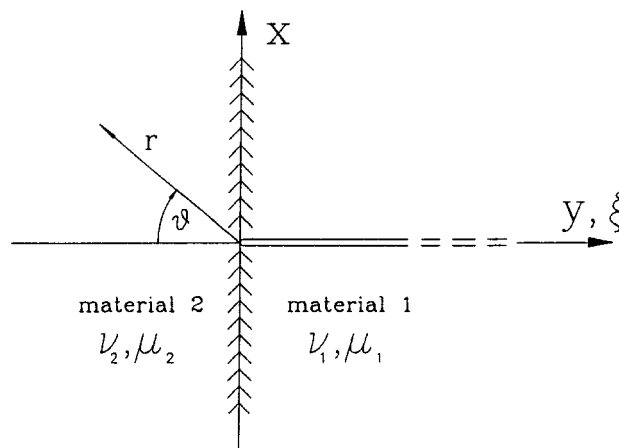


Fig. 1. Semi-infinite crack terminating at a bimaterial interface.

The stress field can be obtained by differentiation of the Airy stress functions, and the strain and displacement fields can be determined using Hooke's law and integration, respectively [3]. The eight constants (four for each half-plane) $A_j^{(i)}$ are determined for the following equilibrium, displacement continuity, and crack traction conditions

$$\begin{aligned}
 \sigma_{\theta\theta}^{(1)}(r, \pi) &= \sigma_{r\theta}^{(1)}(r, \pi) = 0, \\
 \sigma_{\theta\theta}^{(1)}(r, \frac{1}{2}\pi) &= \sigma_{\theta\theta}^{(2)}(r, \frac{1}{2}\pi), \\
 \sigma_{r\theta}^{(1)}(r, \frac{1}{2}\pi) &= \sigma_{r\theta}^{(2)}(r, \frac{1}{2}\pi), \\
 u_r^{(1)}(r, \frac{1}{2}\pi) &= u_r^{(2)}(r, \frac{1}{2}\pi), \\
 u_\theta^{(1)}(r, \frac{1}{2}\pi) &= u_\theta^{(2)}(r, \frac{1}{2}\pi), \\
 u_\theta^{(2)}(r, 0) &= 0, \\
 \sigma_{r\theta}^{(2)}(r, 0) &= 0.
 \end{aligned} \tag{2}$$

The solution of the resulting eigenvalue problem leads to the characteristic equation for the stress singularity λ

$$\cos(\lambda\pi) = \frac{2(\beta - \alpha)}{(1 + \beta)}(1 - \lambda)^2 + \frac{\alpha + \beta^2}{1 - \beta^2}; \quad 0 \leq \lambda < 1, \tag{3}$$

where α and β are the Dundurs constants [3]

$$\alpha = \frac{\mu_2(\kappa_1 + 1) - \mu_1(\kappa_2 + 1)}{\mu_2(\kappa_1 + 1) + \mu_1(\kappa_2 + 1)}, \quad \beta = \frac{\mu_2(\kappa_1 - 1) - \mu_1(\kappa_2 - 1)}{\mu_2(\kappa_1 + 1) + \mu_1(\kappa_2 + 1)}, \tag{4}$$

$\kappa_i = 3 - 4\nu_i$ for plane strain, and $\kappa_i = (3 - \nu_i)/(1 + \nu_i)$ for plane stress.

Equation (3) was first introduced, using a less compact set of elastic constants, by Zak and Williams [2]. The loci of constant λ in the α, β -plane are shown in Fig. 2. As pointed out by Dundurs [4], this plot shows that for $\alpha \rightarrow 1$ the quantity λ is more sensitive to the mismatch in the Poisson's ratios than to that in the shear moduli; the opposite is true for $\alpha \rightarrow -1$. The corresponding eigenfunctions, $\chi^{(i)}(r, \theta)$, are determined to within one multiplicative constant which is usually expressed in terms of the stress intensity factor, k_i , so that the dominant part of the stress field becomes

$$\frac{\sigma_{\theta\theta}^{(i)}}{\frac{1}{\sqrt{2\pi}} \frac{k_i}{r^\lambda}} = f_{\theta\theta}^{(i)}(\theta; \alpha, \beta); \quad \frac{\sigma_{r\theta}^{(i)}}{\frac{1}{\sqrt{2\pi}} \frac{k_i}{r^\lambda}} = f_{r\theta}^{(i)}(\theta; \alpha, \beta); \quad \frac{\sigma_{rr}^{(i)}}{\frac{1}{\sqrt{2\pi}} \frac{k_i}{r^\lambda}} = f_{rr}^{(i)}(\theta; \alpha, \beta). \tag{5}$$

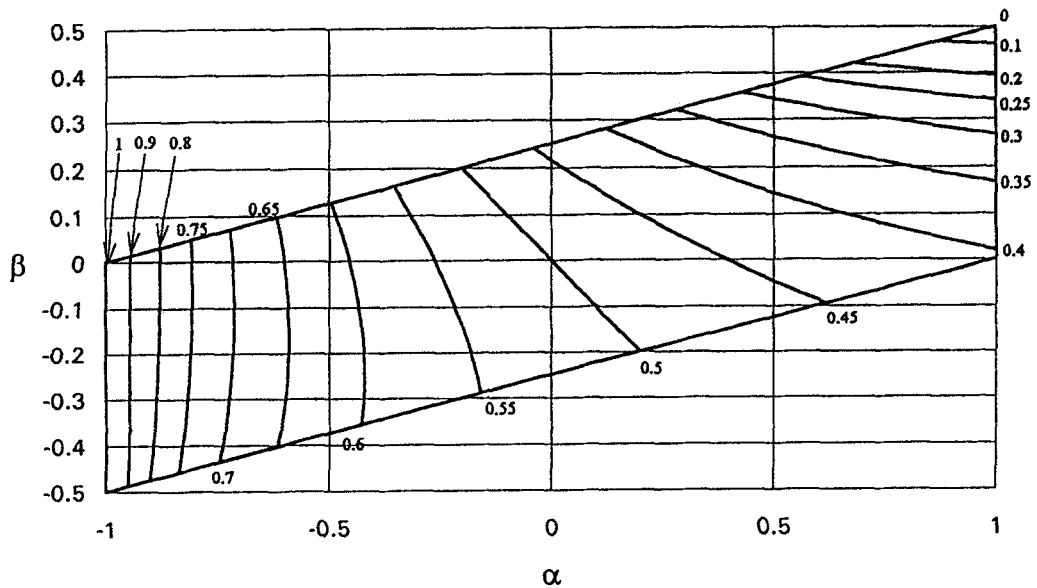
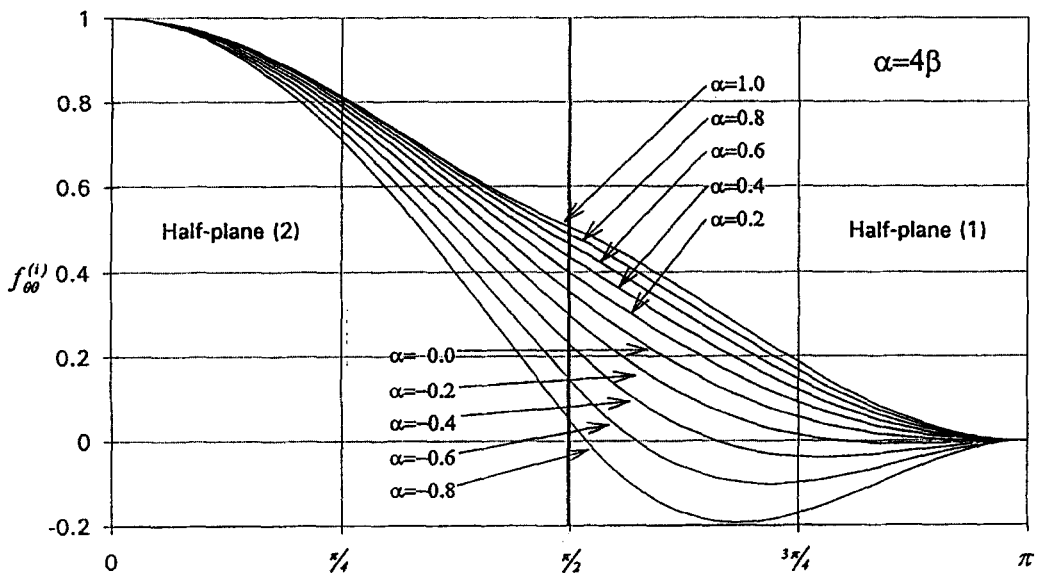


Fig. 2. Loci of constant λ on the $\alpha - \beta$ plane.

Selected plots of $f_{\theta\theta}^{(i)}$, $f_{r\theta}^{(i)}$ and $f_{rr}^{(i)}$ (whose expressions are not presented here) for different values of α and $\beta = 0.25\alpha$ are shown in Figs. 3–5. These particular values of the Dundurs constants were chosen based on Suga's observation [5] that for most of the systems of practical importance the β values range between -0.05 and 0.24 , while the α values span the whole region in the α, β -plane. It is observed that the elastic mismatch has a major influence on the radial stress, as evidenced by the increasingly sharper discontinuity of $f_{rr}^{(i)}$ across the



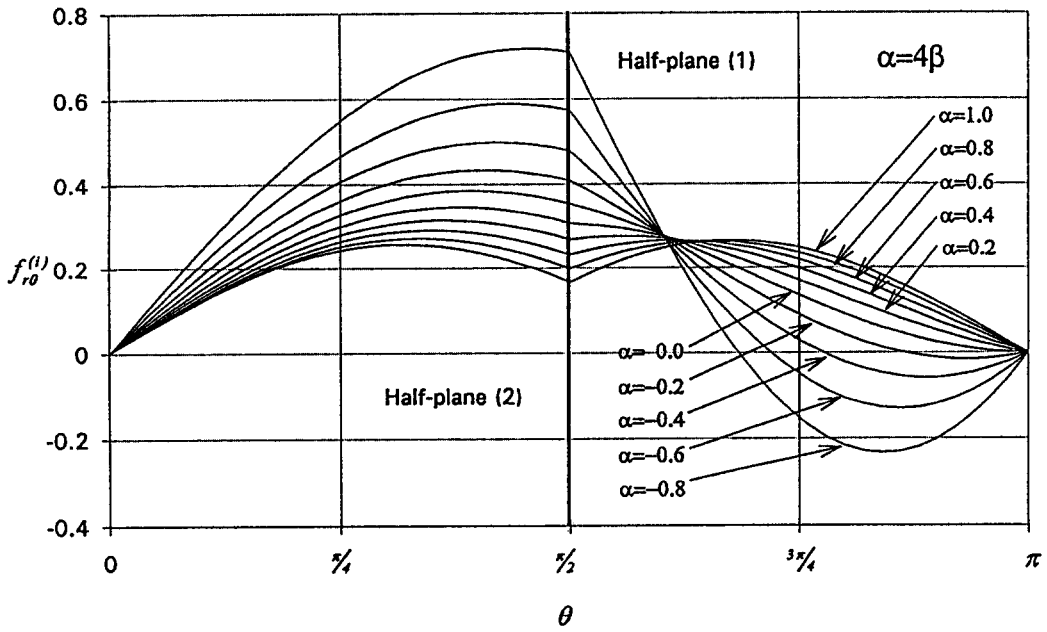


Fig. 4. Angular variation of $f_{r\theta}^{(i)}$ for selected material combinations.

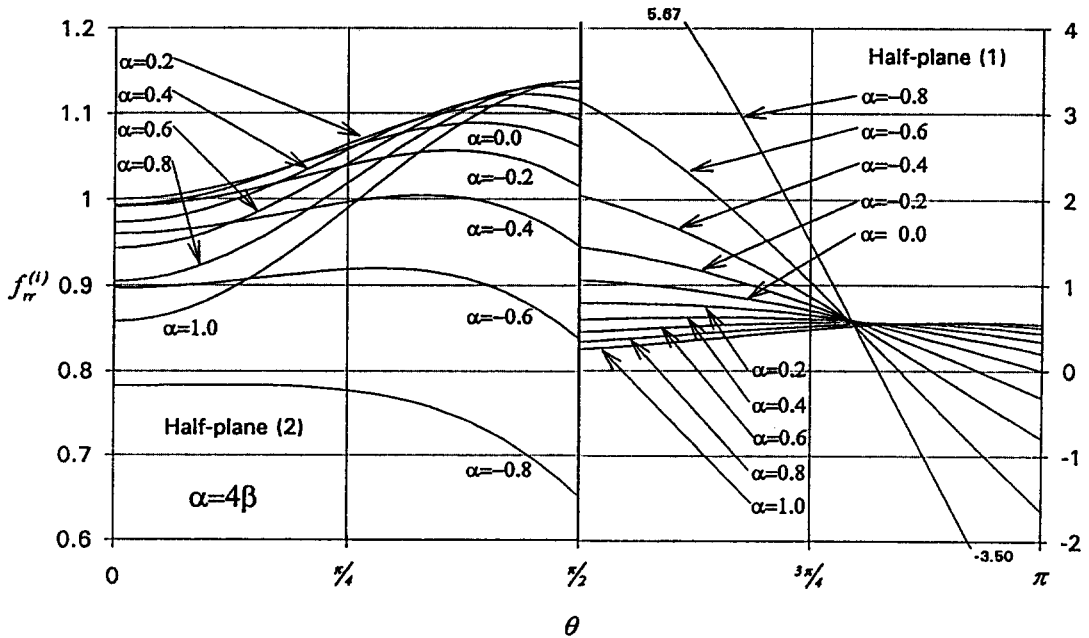


Fig. 5. Angular variation of $f_{rr}^{(i)}$ for selected material combinations.

interface as $|\alpha|$ increases. Furthermore, for relatively large negative values of α , which correspond to the crack being in the stiffer material, a compressive radial stress field develops along the crack faces.

The Von Mises yield criterion, $J_2 = \sigma_0^2/3$, is combined with the asymptotic stress field to estimate the extent of the elastic-plastic boundary in the ductile material of a brittle-ductile

system. In the following, the notation *ductile-brittle system* refers to the case when material 1 is yielding and material 2 is elastic; vice versa for *brittle-ductile system*. The size of the plastic zone in the yielding region, which is a function of the Dundurs constants and the polar angle, is given in non-dimensional form by

$$R_{0,\sigma}^{(i)} \equiv \frac{r_{0\sigma}^{(i)}}{\left[\frac{1}{\sqrt{2\pi}} \frac{k_1}{\sigma_0^{(i)}} \right]^{1/\lambda}} = [f_{\theta\theta}^{(i)2} - f_{\theta\theta}^{(i)} f_{rr}^{(i)} + f_{rr}^{(i)2} + 3f_{r\theta}^{(i)2}]^{1/2\lambda} \quad (6)$$

for plane stress and

$$R_{0,\varepsilon}^{(i)} \equiv \frac{r_{0\varepsilon}^{(i)}}{\left[\frac{1}{\sqrt{2\pi}} \frac{k_1}{\sigma_0^{(i)}} \right]^{1/\lambda}} = [f_{\theta\theta}^{(i)2} - f_{\theta\theta}^{(i)} f_{rr}^{(i)} + f_{rr}^{(i)2} + 3f_{r\theta}^{(i)2} + \nu^{(i)}(\nu^{(i)} - 1)(f_{\theta\theta}^{(i)} + f_{rr}^{(i)})^2]^{1/2\lambda} \quad (7)$$

for plane strain.

A graphic representation of $R_{0,\sigma}^{(i)}$ (plane stress) for $\alpha = 4\beta$ is given in Figs. 6 and 7. Figure 6 corresponds to *brittle-ductile systems* and Fig. 7 corresponds to *ductile-brittle systems*. Analogously, $R_{0,\varepsilon}^{(i)}$ (plane strain) is presented in Figs. 8 and 9 for $\alpha = 4\beta$ and $\nu^{(1)} = \nu^{(2)} = \frac{1}{3}$. A

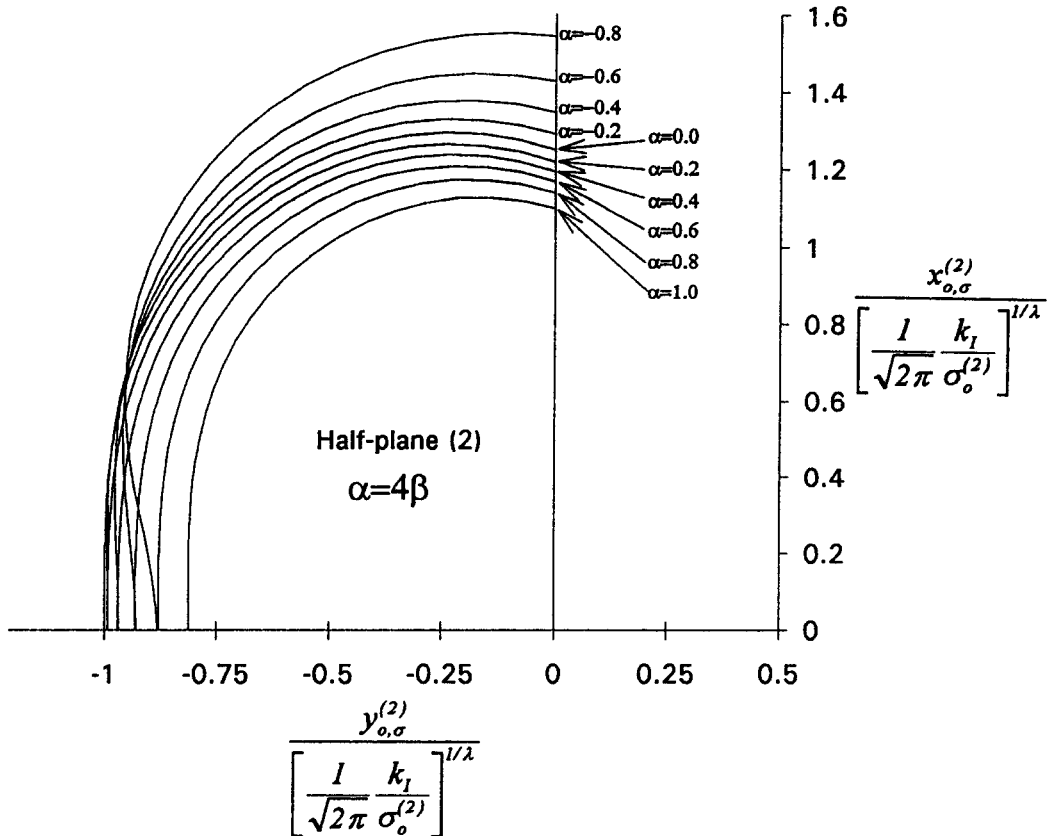


Fig. 6. Contours of $R_{0,\sigma}^{(2)}$ (plane stress) for selected material combinations.

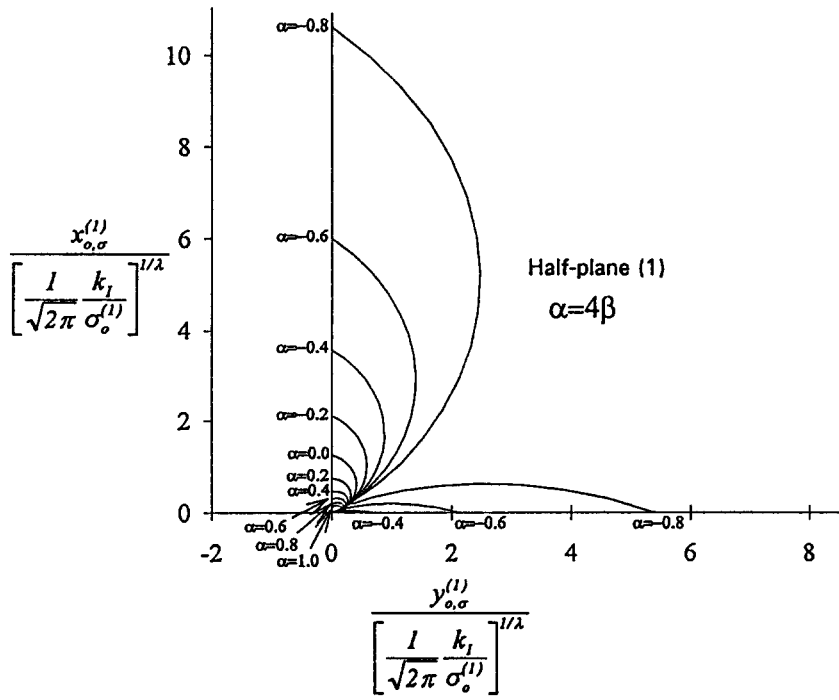


Fig. 7. Contours of $R_{0,\sigma}^{(1)}$ (plane stress) for selected material combinations.

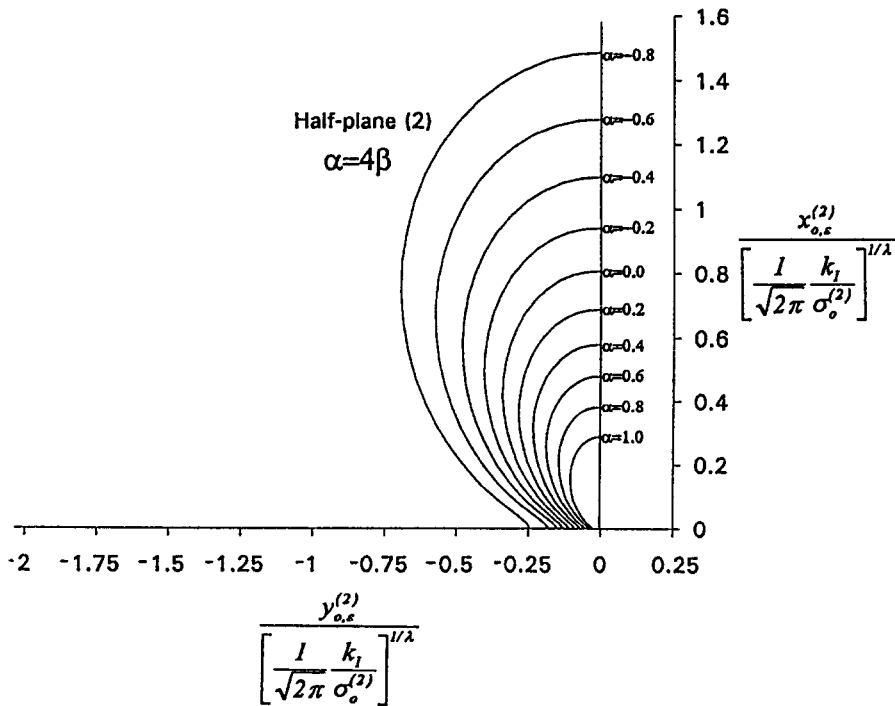


Fig. 8. Contours of $R_{0,\epsilon}^{(2)}$ (plane strain) for selected material combinations.

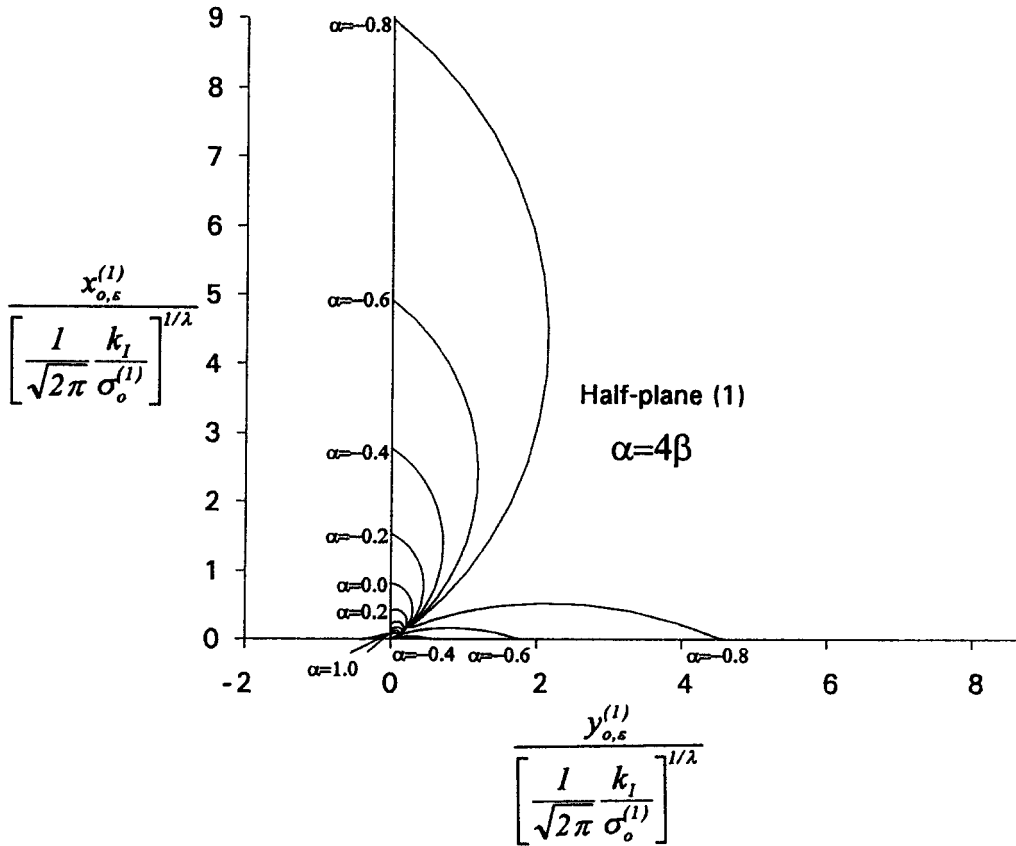


Fig. 9. Contours of $R_{0,\epsilon}^{(1)}$ (plane strain) for selected material combinations.

comparison of Fig. 6 and Fig. 8 shows that the contours of $R_{0,\epsilon}^{(i)}$ are consistently larger than those of $R_{0,\epsilon}^{(j)}$; the difference tends to decrease as $\alpha \rightarrow -1$. However, it is important to note that these plots are not truly indicative of the effects of elastic mismatch on the location of the elastic-plastic boundary, since the stress intensity factor k_I which is strongly dependent on the elastic properties of the bimaterial system, is at this point indeterminate. In order to use (6) and (7) the stress intensity factor must be calculated for a specific crack geometry and applied loading. This is done next for a Griffith crack loaded by uniform pressure.

3. Elastic-plastic boundary for a finite-length crack

Under the assumption of small-scale yielding, (6) and (7) provide a method of estimating the size of the plastic zone induced by finite length cracks, for which a stress intensity factor and a characteristic length are specified.

The problem of a crack of finite length $2a$ (Fig. 10) impinging perpendicularly on the bimaterial interface and loaded by a constant pressure σ can be formulated using the Green's function for the stress along the crack line produced by an edge dislocation. This approach

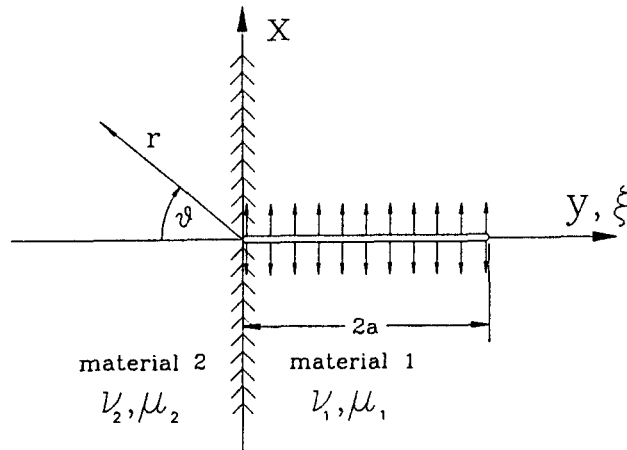


Fig. 10. Crack of length $2a$ loaded by a constant pressure and terminating at the interface.

results in the following system of integral equations [6]

$$\sigma - \frac{2\mu_1}{\pi(\kappa_1 + 1)} \int_0^{2a} b(\xi) \left[\frac{1}{y - \xi} + \frac{\alpha + \beta^2}{1 - \beta^2} \frac{1}{y + \xi} + \frac{2(\alpha - \beta)}{1 + \beta} \frac{\xi(y - \xi)}{(y + \xi)^3} \right] d\xi = 0, \quad 0 \leq y, \xi \leq 2a, \quad (8)$$

$$\int_0^{2a} b(\xi) d\xi = 0,$$

where $b(\xi)$ is the unknown dislocation density, defined in terms of the crack opening displacement $[u_x]$ as $b(\xi) \equiv -\partial[u_x]/\partial\xi$. The first equation (8) is a singular integral equation with a generalized Cauchy kernel that expresses the boundary condition along the crack surfaces, while the second equation is a crack tip closure condition that guarantees a unique solution.

Once the dislocation density $b(\xi)$ is computed by solving the system of equations (8), the stress field ahead of the crack (material 2) is given by

$$\sigma_{xx}^{(2)}(y, 0) = \frac{2\mu_1}{\pi(\kappa_1 + 1)} \frac{1 + \alpha}{1 - \beta^2} \int_0^{2a} b(\xi) \left[\frac{2\beta + 1}{\xi - y} + \frac{2\beta x}{(\xi - y)^2} \right] d\xi, \quad 0 \leq y, \xi \leq 2a. \quad (9)$$

The analysis of the behavior of the generalized Cauchy kernel in (9) using the Muskhelishvili technique [7] yields the expression for the non-dimensional stress intensity factor $h(\alpha, \beta)$

$$h(\alpha, \beta) = \frac{k_1}{\sigma \sqrt{\pi a^\lambda}} = \psi \frac{\kappa_1 + 1}{2\mu_1} \hat{b}(0); \quad (10)$$

$$\psi \equiv \frac{2\mu_1}{\kappa_1 + 1} \frac{1}{\sin(\lambda\pi)} \left(\frac{1 + \alpha}{1 - \beta^2} \right) [1 - 2\beta(\lambda - 1)],$$

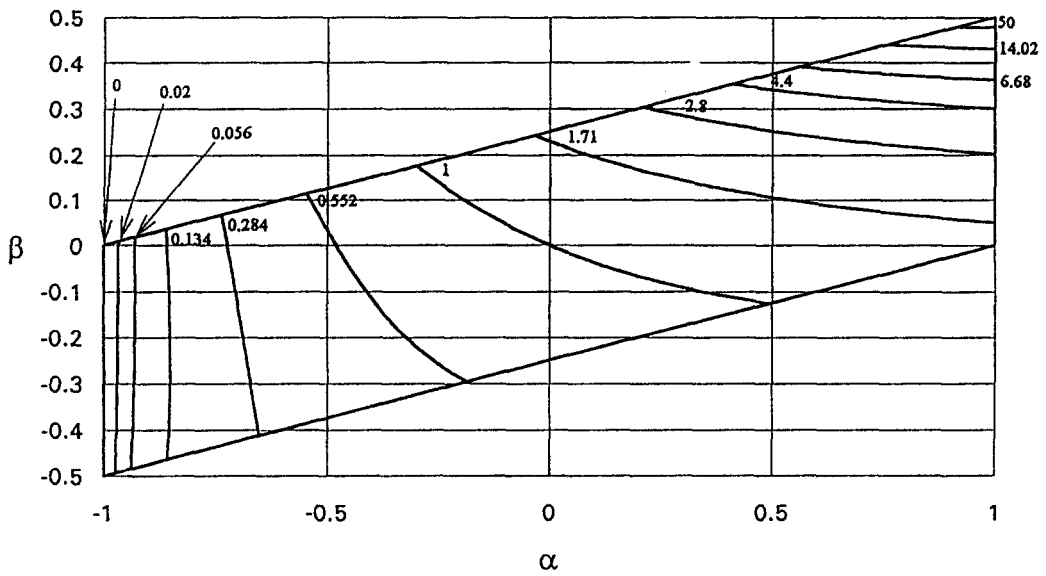


Fig. 11. Loci of constant h in $\alpha - \beta$ plane.

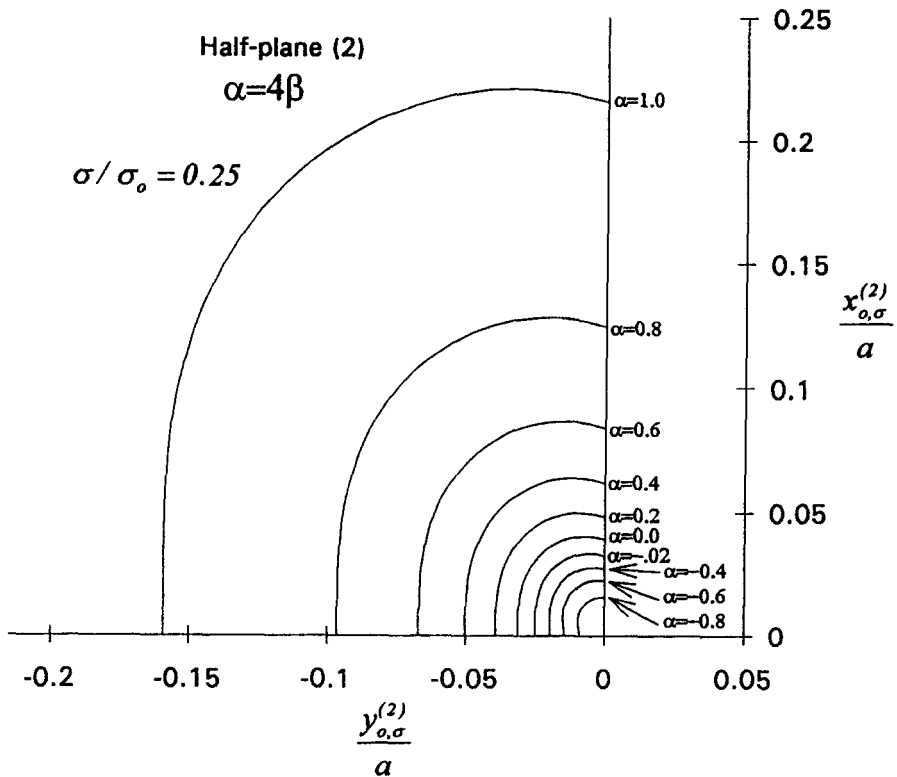


Fig. 12. Elastic-plastic boundary in material 2 (brittle-ductile system) for selected material combinations and plane stress conditions.

where $\hat{b}(\xi) = a^{-(1/2+\lambda)} b(\xi) \xi^\lambda (2a - \xi)^{1/2}$ is the regular part of the dislocation density. Upon substitution into (6) and (7), the radius of the plastic zone in the yielding material normalized by the characteristic length of the problem, a , becomes

$$\frac{r_{0,\sigma}^{(i)}}{a} = \left[\frac{h(\alpha, \beta)}{\sqrt{2}} \frac{\sigma}{\sigma_0^{(i)}} f^{(i)}|_\sigma \right]^{1/\lambda} \quad \text{plane stress;} \tag{11}$$

$$\frac{r_{0,\varepsilon}^{(i)}}{a} = \left[\frac{h(\alpha, \beta)}{\sqrt{2}} \frac{\sigma}{\sigma_0^{(i)}} f^{(i)}|_\varepsilon \right]^{1/\lambda} \quad \text{plane strain;} \tag{12}$$

The singular integral equation was solved numerically using two techniques: the first approximated $\hat{b}(\xi)$ with Jacobi polynomials [6], and the second with piecewise quadratic polynomials [8]. The results presented subsequently represent an agreement between the two methods to three significant figures.

Equations (11) and (12) show that the stress intensity factor and the strength of the singularity play a key role in the location of the elastic-plastic boundary. The loci of equal h in the α, β -plane are shown in Fig. 11. A comparison of Fig. 11 and Fig. 2 shows that higher values of α (or of the ratio μ_2/μ_1) are associated with large values of h and smaller values of λ . Therefore, within the limits of small scale yielding conditions, two competing mechanisms contribute to the size of the plastic zone as the stiffness of material 2 is increased relative to the stiffness of

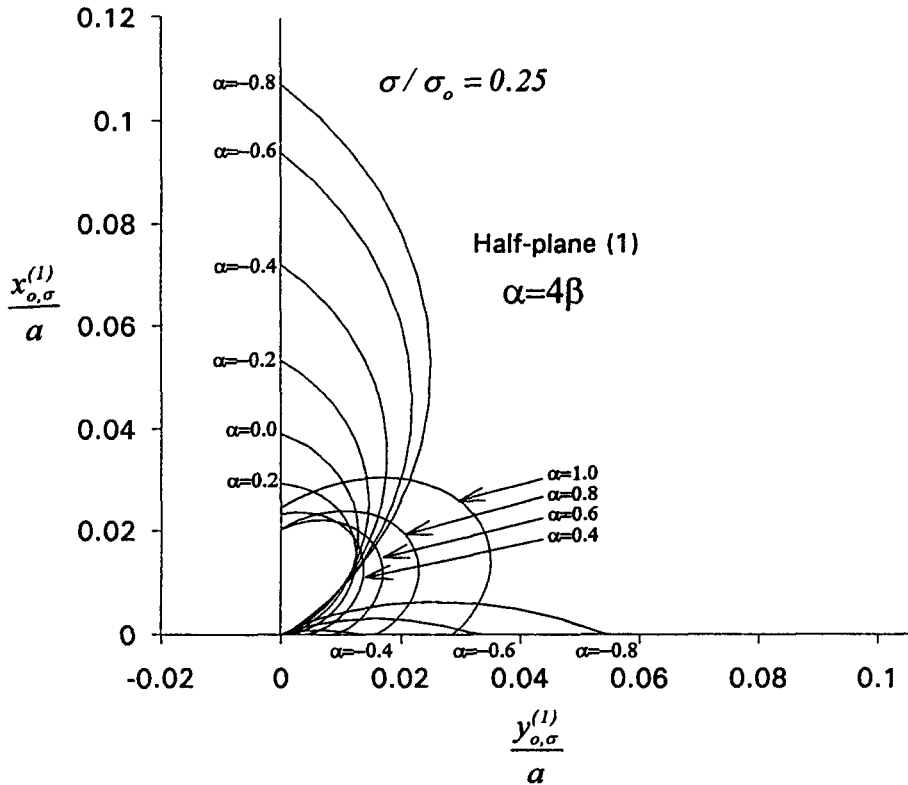


Fig. 13. Elastic-plastic boundary in material 1 (ductile-brittle system) for selected material combinations and plane stress conditions.

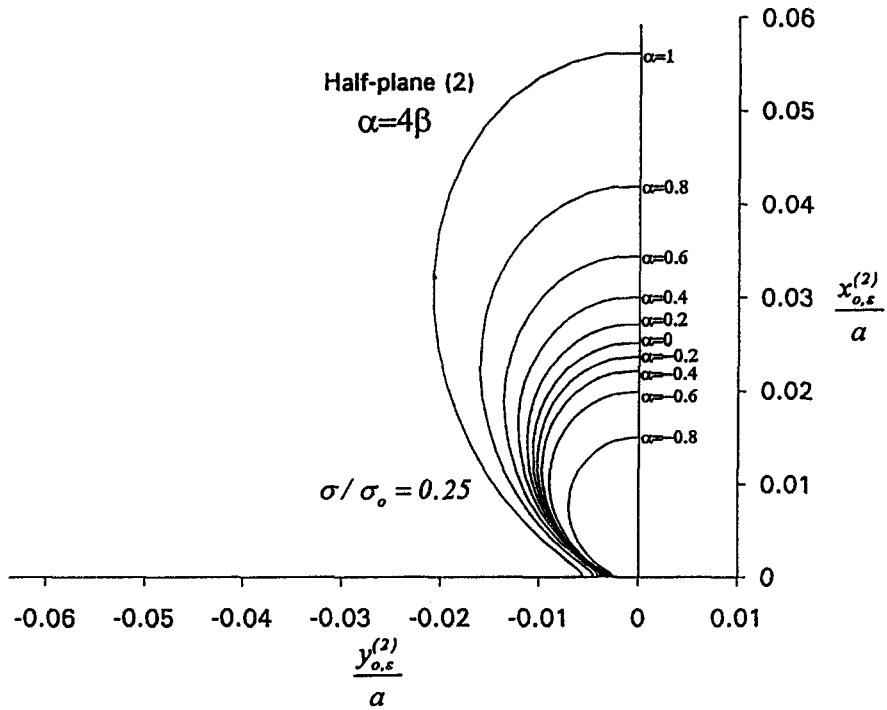


Fig. 14. Elastic-plastic boundary in material 2 (brittle-ductile system) for selected material combinations and plane strain conditions.

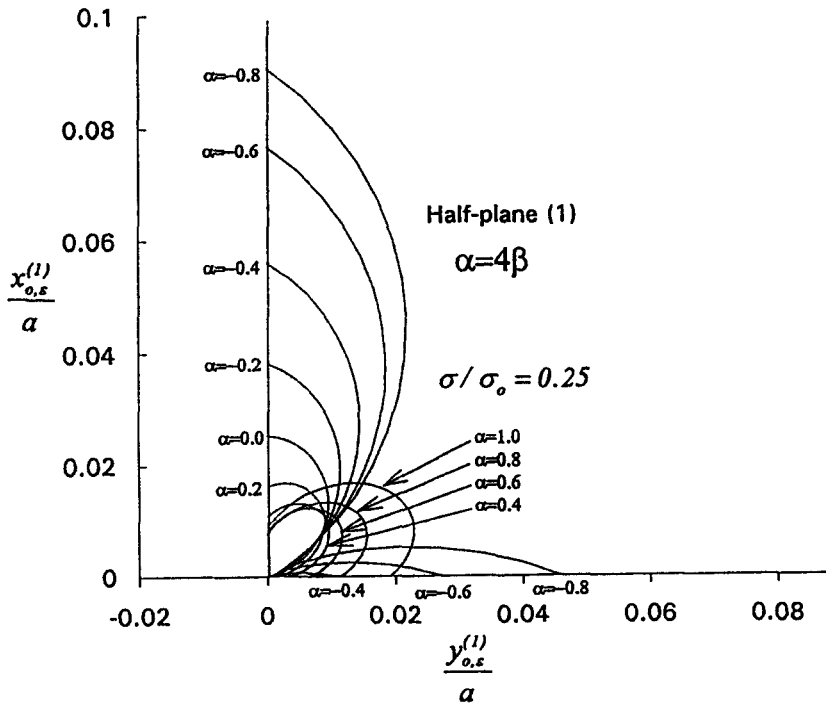


Fig. 15. Elastic-plastic boundary in material 1 (ductile-brittle system) for selected material combinations and plane strain conditions.

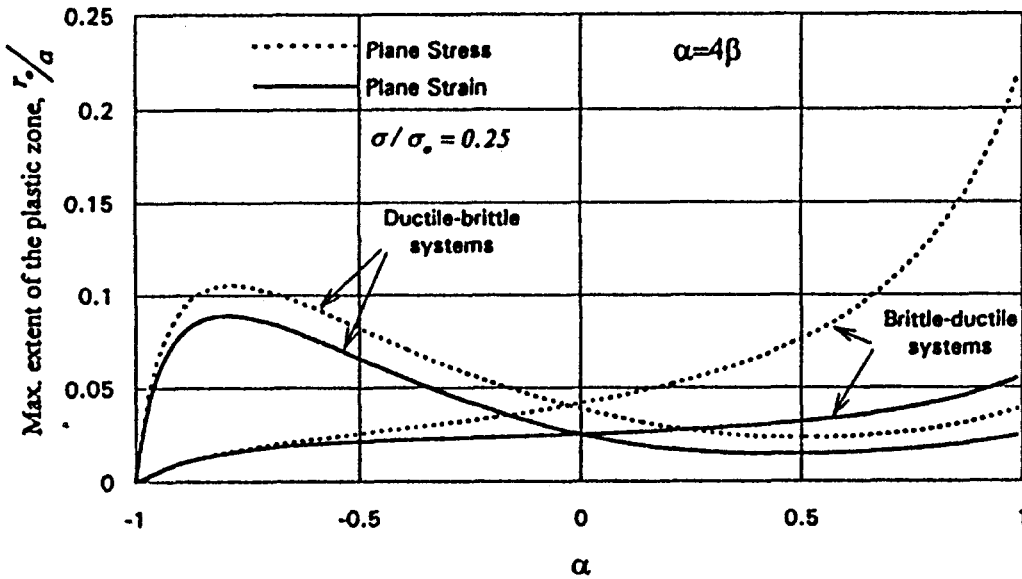


Fig. 16. Maximum extent of the plastic zone in the yielding material for different bimaterial systems.

material 1; while the stress intensity factor tends to increase, the strength of the crack tip singularity decreases.

The dependence of $r_{0,\sigma}^{(i)}$ (plane stress) on the elastic mismatch is shown in Figs. 12 and 13 for selected values of $\alpha = 4\beta$ and $\sigma/\sigma_0 = 0.25$. These plots clearly show that the extent of the elastic-plastic boundary for a brittle-ductile system (Fig. 12) is a strong monotonically increasing function of α . However, for a ductile-brittle system (Fig. 13) the scenario is complicated as a result of the compressive radial stress field. In particular, in the latter case the plastic zone expands rapidly as α increases from -1 to ~ -0.8 and then it tends to decrease. Note that in the limit as $\alpha \rightarrow -1$ or $\mu_2/\mu_1 \rightarrow 0$ (which means that the crack has reached a free surface), the stress intensity factor approaches zero as well as the size of the plastic zone. The ratio $\sigma/\sigma_0 = 0.25$ was chosen so that small-scale yielding conditions hold for the case of a homogeneous system ($\alpha = \beta = 0$).

The elastic-plastic boundary for plane strain conditions is plotted in Figs. 14 and 15, where again $\sigma/\sigma_0 = 0.25$, $\alpha = 4\beta$ and $\nu^{(1)} = \nu^{(2)} = \frac{1}{3}$. Considerations similar to the ones made for plane stress conditions hold also for this case. As expected, the size of the plastic zone is larger for plane stress than for plane strain.

The maximum size of the plastic zone in the ductile component as a function of $\alpha = 4\beta$ for plane stress and plane strain is shown in Fig. 16, in which $\sigma = 0.25\sigma_0$. Note that Fig. 16 presents for each value of α the corresponding maximum extent of the plastic zone, which may occur at different polar angles, depending on the level of elastic mismatch.

4. Conclusions

The location of the boundary of the plastic zone induced by a finite length crack perpendicular to a bimaterial interface is very sensitive to the elastic properties of the two bonded half-planes. The key parameters that control the relative size of the yielded region are the stress intensity

factor k_1 and the strength of the crack tip singularity λ . Within the limits of small-scale yielding, as the relative stiffness of the two bonded materials varies, k_1 and λ have competing effects on the size of the plastic zone. The extent of yielding ahead of the crack increases with increasing μ_2/μ_1 , which corresponds to the material ahead of the crack being stiffer than the one in which the crack is.

References

1. Ming Y. He, R.M. McMeeking and Ning T. Zhang, *Materials Research Society Symposium Proceedings* 239 (1992) 585–590.
2. A.R. Zak and M.L. Williams, *Journal of Applied Mechanics* 30 (1963) 142–143.
3. J. Dundurs, in *Mathematical Theory of Dislocations*, ASME (1969) 70–114.
4. J. Dundurs, *Scripta Metallurgica* 4 (1970) 313–314.
5. T. Suga, G. Elssner and S. Schmauder, *Journal of Composite Materials* 22 (1988) 917–934.
6. F. Erdogan, G.D. Gupta and T.S. Cook, in *Mechanics of Fracture* 1, G.C. Sih (ed.) Noordhoff International Publishing, 368–425.
7. N. Muskhelishvili, *Singular Integral Equations*, P. Noordhoff, Groningen, Holland (1953).
8. G.R. Miller and L.M. Keer, *Quarterly of Applied Mathematics* 42 (1985) 455–465.